RSC Advances

PAPER

View Article Online
View Journal | View Issue

Open Access Article. Published on 05 March 2018. Downloaded on 10/19/2025 7:44:04 PM.
This article is licensed under a Creative Commons Attribution-NonCommercial 3.0 Unported Licence.

Check for updates

Cite this: *RSC Adv.*, 2018, **8**, 9364

Sorption characteristics of *N*-acyl homserine lactones as signal molecules in natural soils based on the analysis of kinetics and isotherms

Hongjie Sheng,[ab] Fang Wang,*[ab] Chenggang Gu,[a] Robert Stedtfeld,[c] Yongrong Bian,[a] Guangxia Liu,[ab] Wei Wu[ab] and Xin Jiang[ab]

Quorum sensing, the communication between microorganisms, is mediated by specific diffusible signal molecules. Adsorption is an important process that influences the transport, transformation and bioavailability of *N*-acyl homoserine lactone (AHL) in complex natural environments such as soil. To examine the adsorption characteristics of *N*-hexanoyl, *N*-octanoyl, *N*-decanoyl and *N*-dodecanoyl homoserine lactones in soil, equilibrium and kinetic experiments were conducted in two types of soils (oxisol and alfisol) and monitored using Fourier-transform infrared spectroscopy (FTIR). A pseudo-second-order equation accurately described the sorption kinetics of AHLs in the two soils ($R^2 \geq 0.97$, NSD $\leq$ 21.25%). The AHL sorption reached equilibrium within 24 h and 12 h for oxisol and alfisol, respectively. The sorption kinetics of AHLs adsorbed on the soils were fitted to the Boyd model, suggesting that film diffusion was the rate-limiting process. Partition played a more vital role than surface adsorption in the AHL adsorption process. The adsorption isotherms of AHLs could be described by the Langmuir and Freundlich equation ($R^2 \geq 0.98$), indicating that the sorption process involved monolayer sorption and heterogeneous energetic distribution of active sites on the surfaces of the soils. The thermodynamic parameter, Gibbs free energy (ΔG), and a dimensionless parameter showed that the sorption of AHLs was mainly dominated by physical adsorption. Additionally, according to the FTIR data, the electrostatic forces and hydrogen bonding possibly influenced the adsorption of AHLs on the above mentioned two soils. The sorption characteristics of AHLs in soils correlated well with the molecular structure, solubility speciation and log *P* (*n*-octanol/water partition coefficient) of AHLs.

Received 20th September 2017
Accepted 19th February 2018

DOI: 10.1039/c7ra10421a

rsc.li/rsc-advances

1. Introduction

Quorum sensing (QS) is a mechanism for intracellular or intercellular communication among microorganisms in response to a variation in the community density with the objective of coordinating their population behavior and controlling gene expression.[1–3] QS is mediated by the synthesis, release and perception of small signal molecules.[4,5] When the concentration of a signal molecule reaches a threshold level, it plays an important role in regulating gene expressions and coordinating biological functions such as bioluminescence,[6–8] antibiotic biosynthesis,[9–11] bacteria motility,[12] and biofilm development.[13–15] For example, recent studies have shown that the degradation of 1,2,4-trichlorobenzene can be regulated by the conduction of signal molecules.[15,16]

N-Acyl homoserine lactones (AHLs) are often employed by Gram-negative bacteria as signal molecules.[16] An AHL consists of a five-membered ring containing amide-linked side chains, and the side chains are identified by a range of 4–18 carbons in length.[17] The structure of AHLs determines not only their signaling function but also their modes of interaction with environmental factors during cell-to-cell transit.[17] Soil microorganisms communicate with each other through quorum sensing to elicit beneficial or pathogenic effects on plant development and productivity.[18,19] Previous studies have reported that AHLs can be biodegraded by a wide range of organisms with the enzymatic capabilities.[15,20–22] Some AHLs undergo isomerization to produce metal chelators,[23] which bind iron in the *Pseudomonas aeruginosa* culture. Hydrolysis of AHLs occurs during bacterial growth and is dependent on the pH, temperature and length of the acyl chains.[24] AHL hydrolysis can occur readily in biochar, which is generally alkaline,[24] whereas AHLs are much more stable in acidic soil. However, it is worth noting that the biodegradation of AHLs plays a more important role than hydrolysis in natural soils.[25] Furthermore, soil is one of the most important sources for accumulation and diffusion of biomolecules such as peptides and fatty acids.[26,27] Sorption

[a]*Key Laboratory of Soil Environment and Pollution Remediation, Institute of Soil Science, Chinese Academy of Sciences, Nanjing 210008, China. E-mail: wangfang@issas.ac.cn; Fax: +86 25 86881000; Tel: +86 25 86881350*

[b]*University of the Chinese Academy of Sciences, Beijing 100049, China*

[c]*Department of Civil and Environmental Engineering, Michigan State University, East Lansing, Michigan 48824, USA*

This journal is © The Royal Society of Chemistry 2018

Open Access Article. Published on 05 March 2018. Downloaded on 10/19/2025 7:44:04 PM.
This article is licensed under a Creative Commons Attribution-NonCommercial 3.0 Unported Licence.

on the soil particles (mainly on soil organic matter) influences the mobility, fate and bioavailability of biomolecules.[28,29] Therefore, the physicochemical properties of soil might affect the mobility and stability of AHLs and reduce their bioavailability to bacteria. The bioavailability of biomolecules is linked to the biodegradation of AHLs as this results in the consumption of signal molecules by other microbes. Charcoal may disrupt AHL-mediated cell–cell communication by decreasing the level of bioavailable AHL through a combination of signal sorption and pH-dependent hydrolysis of the lactone ring.[30] Biochar inhibition of microbial communication by the sorption of 3-oxo-C_{12}-HSL varies with the properties associated with the biochar, especially the surface area.[31] Adsorption of 3-oxo-C_{12}-HSL lactone onto colloidal minerals is mainly dominated by hydrogen bonding and hydrophobic interactions.[29] Therefore, sorption of AHLs on soil is likely to mediate the diffusion and bioavailability of AHLs in the soil, thus influencing cell–cell communication. However, there are still gaps in the understanding of the sorption behavior of AHLs in soil.[25]

The objectives of the present study are as follows: (1) to investigate the sorption behavior of AHLs on two different natural soils using kinetics and isotherms, (2) to understand the relationship between AHL adsorption characteristics and physicochemical properties. *N*-Hexanoyl, *N*-octanoyl, *N*-decanoyl, and *N*-dodecanoyl homoserine lactones (C_6-, C_8-, C_{10}- and C_{12}-HSL) are selected as model AHLs since they represent short, medium and long acyl chain AHLs with different physicochemical properties in the natural environment. Sorption kinetic and isotherm experiments of AHLs are conducted using two types of soil.

2. Material and methods

2.1. Chemicals and soils

Standard samples (purity > 99.9%) of *N*-hexanoyl (C_6-HSL), *N*-octanoyl (C_8-HSL), *N*-decanoyl (C_{10}-HSL) and *N*-dodecanoyl homoserine lactones (C_{12}-HSL) with varying physiochemical properties (Table 1) were obtained from Sigma-Aldrich (Buchs, Switzerland). Ethyl acetate was purchased from Merck (Darmstadt, Germany). The stock solution was prepared by the dissolution of samples in ethyl acetate at a concentration of 1000 mg L^{-1} and stored at −20 °C. All chemical reagents were of analytical grade or better.

2.2. Soil sampling

The inactivation of AHLs was discovered to be a consequence of the pH-dependent hydrolysis of the lactone ring, *etc.* in alkaline pH conditions.[24,30,32] Hydrolysis of AHLs easily occurred in alkaline soil, whereas in acidic soil AHLs were much more stable.[24] Oxisol (S1) and alfisol (S2), which are widely distributed in Southern China, having different textures and organic matter content with pH value lower than 7.0 were used in the sorption experiments. The soils were classified according to the triangular diagram textures of the United States Department of Agriculture. Soil S1 was sampled from grasslands in Jinjiang, Hainan, China (19°46′16.6″ N, 110°00′21.5″ E), and soil S2 was sampled from an agricultural field in Baguazhou, Nanjing, China (32°12′4.6″ N, 118°50′112.3″ E). The soils were collected from the depths of 0–20 cm, air dried and passed through a 2 mm metallic sieve before being stored at 4 °C. The soil pH was determined by a pH meter in a solution of 0.01 M $CaCl_2$ with a soil/liquid ratio of 1 : 2. The percentages of sand, silt, and clay in the soil samples were analyzed using a Bouyoucos densitometer. The total organic carbon content was quantified by the dry combustion method.[33] The total amount of organic matter in each soil (% OM) was calculated by multiplying the organic carbon content (% OC) by 1.724 considering that carbon accounts for 58% of the soil organic matter.[34] The physicochemical properties of AHLs are summarized in Table 2. C_6, C_8, C_{10}, and C_{12}-HSL in both soils were quantified with GC/MS as described previously and were all lower than 2.53 μg kg^{-1} (Table 1).[35]

2.3. Sorption kinetics of AHLs on soil

Batch experiments were performed in triplicate to investigate the sorption of AHLs onto the soils. Aliquots (50 mg) of sterilized soils were weighted into 20 mL glass tubes with Teflon-lined screw caps to avoid the loss of AHLs during sorption. A 5 mL aqueous solution containing 0.01 M $CaCl_2$ was added to

Table 1 The physicochemical properties and concentrations of *N*-acyl homoserine lactones (HSLs) in soil

AHLs	Molecular weight (Da)	Water-solubility (mg L^{-1})	Polarity	log P^a	Chemical structure	Concentration in S1 (μg kg^{-1})	Concentration in S2 (μg kg^{-1})
N-Hexanoyl HSL C_6-HSL	199.3	1.48×10^4	5.81	1.02	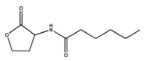	1.30 ± 0.27	2.53 ± 0.03
N-Octanoyl HSL C_8-HSL	227.3	1.53×10^3	6.19	1.97	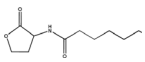	1.78 ± 0.25	ND[b]
N-Decanoyl HSL C_{10}-HSL	255.4	1.55×10^2	5.90	2.96	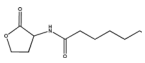	1.69 ± 0.04	ND[b]
N-Dodecanoyl HSL C_{12}-HSL	283.4	15.62	6.44	4.02	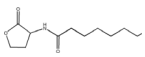	ND[c]	ND[c]

[a] log *P* is *n*-octanol/water partition coefficient representing the analyte's hydrophobicity.[32] [b] ND means lower than 1.0 μg kg^{-1}. [c] ND means lower than 1.25 μg kg^{-1}.

Open Access Article. Published on 05 March 2018. Downloaded on 10/19/2025 7:44:04 PM.
This article is licensed under a Creative Commons Attribution-NonCommercial 3.0 Unported Licence.

Table 2 Physicochemical properties of the soils

Sample no.	Soil information	pH	Clay (%)	Silt (%)	Sand (%)	OM[a] (%)
S1	Oxisol	5.87 ± 0.07	36.20 ± 2.35	30.64 ± 3.64	33.16 ± 2.15	2.81 ± 0.72
S2	Alfisol	6.97 ± 0.12	31.01 ± 1.97	57.54 ± 5.23	11.45 ± 1.63	3.19 ± 0.59

[a] OM means organic matter content.

the glass tubes to maintain a relatively constant ionic strength. To avoid the biodegradation of AHLs,[21,22,36] 100 M $HgCl_2$ was added to each tube to inhibit microbial activity. Ten μL AHL stock solution (1000 mg L^{-1}) in ethyl acetate was spiked to give a final concentration of 2.0 mg L^{-1}, leaving the final methanol concentration under 0.1% (v/v) to avoid co-solvent effect. Control experiments with no addition of sorbents (S1 and S2) were used to evaluate the possible loss of AHLs *via* interaction with tubes and filters as well as abiotic/biotic degradation. Abiotic degradation occurred at an alkaline pH and room temperature.[17,37,38] The longer the acyl side chain and the lower the pH the more stable are the AHL signals.[24] The pH value of soil S1 set was 6.0, at which the abiotic degradation half-lives of C_8-, C_{10}-HSL were 57 days and 55 days, respectively.[32] The original pH in the control and in the soil S2 sets were 6.7 and 6.8, respectively. These were adjusted to 6.0 using HCl to minimize the chemical hydrolysis of AHLs. All the sealed glass tubes were shaken at 120 rpm on a SHZ-28A vibrator (Baidian company, Shanghai, China) at 25 ± 0.5 °C in darkness for 0.5, 1, 2, 4, 6, 8, 12, 24 and 48 h. All sets were run in triplicate and sampled for AHL analyses at each time point.

2.4. Sorption isotherms of AHLs on soil

Sorption isotherms of AHLs were conducted with 50 mg of sterilized soil, and samples were prepared in 5 mL $CaCl_2$ and $HgCl_2$ solution, as in Section 2.2, with varying amounts of AHLs (0.1, 0.5, 1, 2 or 5 mg L^{-1}). As in the above mentioned data the control without sorbents (S1 and S2) was used to evaluate loss of AHLs. The initial pH in all the sets was adjusted to 6.0 using HCl. All the bottles were incubated in a vibrator (120 rpm, 25 °C) in darkness for 24 h (S1) and 12 h (S2). At the end of the experiment, all the tubes were sampled for AHL analysis. All sets were run in triplicate.

2.5. Extraction and analysis of AHLs

The aqueous solutions (1.5 mL) from the 20 mL Teflon centrifuge tubes were transferred into 2 mL centrifuge tubes and centrifuged at 12 000 rpm for 5 min. Next, 0.5 mL supernatant was added into a 2 mL centrifuge tube with 1 mL ethyl acetate, vortexed for 2 min and centrifuged at 12 000 rpm for a further 2 min. Then, 0.8 mL of the ethyl acetate phase was added into a 2 mL centrifuge tube containing 1 g anhydrous sodium sulfate, vortexed and centrifuged as mentioned above. Finally, 0.5 mL supernatant was transferred into a GC vial. To minimize the system errors (such as sorption effect of the glass bottles and the fiberglass films, *etc.*), all the control samples were analyzed using the same extraction procedure as mentioned above.

The samples were analyzed by an Agilent 7890A GC system equipped with an Agilent 5975C mass selective detector (Agilent, USA) and an HP-5MS column (30 m, 0.250 mm i.d., 0.25 μm) according to a previously published procedure.[35] The sample injection was done in split mode (split ratio 5 : 1). Helium (99.999%) was used as the carrier gas at a constant flow rate of 1 mL min^{-1}. The GC inlet temperature was set at 290 °C. The oven temperature was ramped up from 100 °C to 150 °C at a rate of 35 °C min^{-1} and then increased by 15 °C min^{-1} to 280 °C before being held at 280 °C for 6 min. The mass spectrometry conditions were as follows: electron ionization source (70 eV), MS quad (150 °C), MS source (230 °C) and solvent delay (3.6 min). The mass spectrometer was run in SIM mode at m/z = 143. The AHL concentrations were quantified with a freshly prepared working solution using authentic standards.

2.6. Fourier transform infrared spectroscopy (FTIR) analysis

All the samples were measured with FTIR before and after the AHLs sorption (Section 2.3) to elucidate the sorption mechanism. The four treatments included (a) oxisol, (b) AHLs with oxisol, (c) alfisol, and (d) AHLs with alfisol. The samples were centrifuged and freeze-dried before FTIR analysis.[39] 1 mg of the solid constituent was gently mixed with 200 mg KBr and oven-dried at 108 °C, followed by pressing the mixture into a pellet. The FTIR spectrum was obtained using a NEXUS 870 spectrophotometer (Thermo Nicolet, Madison, USA) with a resolution of 4 cm^{-1} and scanning from 4000 to 400 cm^{-1}.

2.7. Quality control and data analysis

The recovery experiments of C_6-, C_8-, C_{10}- and C_{12}-HSL with no addition of soils were prepared and analyzed using the same procedure as mentioned previously (Section 2.3). AHL was extracted and analyzed by GC-MS as described previously (Section 2.5).

Several sorption kinetics models (pseudo-first-order, pseudo-second-order, Elovich and intra-particle diffusion equations) and isotherm sorption models (Langmuir model and Freundlich equations) were fitted to the experimental data, further elucidating the sorption rate limiting step and the relevant sorption mechanisms.

2.7.1. Sorption kinetics. When adsorption occurs by diffusion through a boundary, the kinetics of the process can be depicted by the pseudo-first-order (eqn (1)),[40] pseudo-second-order (eqn (2))[41] and Elovich eqn (3):[42]

Open Access Article. Published on 05 March 2018. Downloaded on 10/19/2025 7:44:04 PM.
This article is licensed under a Creative Commons Attribution-NonCommercial 3.0 Unported Licence.

$$q_t = q_e(1 - \exp(-k_1 t)) \quad (1)$$

$$q_t = \frac{k_2 q_e^2 t}{1 + k_2 q_e t} \quad (2)$$

$$q_t = a + b \ln(t) \quad (3)$$

Here, k_1 (kg (mg h)$^{-1}$) is the adsorption rate constant, q_e (mg kg^{-1}) is the adsorption amount at equilibrium time, and q_t (mg kg^{-1}) is the adsorption amount on the soil surface at time t. k_2 (kg (mg h)$^{-1}$) is the sorption rate constant of pseudo-second-order equation. a (mg kg^{-1}) and b are the constants related to the extent of surface coverage and activation energy for chemisorption, respectively.

Intra-particle diffusion (*i.e.* Weber and Morris model)[43] and Boyd (eqn (5)) models[44] were further used to elucidate the sorption process and verify whether the sorption rate was controlled by film diffusion or intra-particle diffusion process:

$$q_t = k_i t^{1/2} + C_i \quad (4)$$

$$B_t = -0.4977 - \ln(1 - F) \quad (5)$$

Here, k_i (mg (kg t$^{1/2}$)$^{-1}$) is the intra-particle diffusion rate constant, and C_i (mg kg^{-1}) represents the thickness of the boundary layer. $F = q_t/q_e$ indicates the fractional attainment of equilibrium at time t (h).

The normalized standard deviation (NSD) was calculated to further quantitatively verify the suitability of the kinetic model using the following equation:

$$\mathrm{NSD} = 100\sqrt{\frac{\sum\left[\left(q_{t,\mathrm{exp}} - q_{t,\mathrm{cal}}\right)/q_{t,\mathrm{exp}}\right]^2}{i-1}} \quad (6)$$

Here, $q_{t,\mathrm{exp}}$ and $q_{t,\mathrm{cal}}$ refer to the experimental and calculated values, respectively, and i is the number of data points.

2.7.2. Sorption isotherms. Freundlich[45] and Langmuir[46] isotherm models were employed to fit the equilibrium data:

$$q_e = k_F C_e^{1/n} \quad (7)$$

$$q_e = \frac{q_m k_L C_e}{1 + k_L C_e} \quad (8)$$

Here, k_F and n are Freundlich constants related to the sorption capacity and intensity, respectively. q_m (mg g^{-1}) is the maximum sorption capacity of adsorbent, and k_L (L mg^{-1}) is the Langmuir constant related to rate adsorption.

Based on the further analysis of Langmuir equation, the dimensionless parameter of the equilibrium or sorption intensity (R_L) can be calculated using the following equation:[47]

$$R_L = \frac{1}{1 + K_L C_0} \quad (9)$$

Here, C_0 (mg L^{-1}) is the highest initial concentration of AHLs, and K_L (L mg^{-1}) is Langmuir constant. The parameter R_L, the indicator of the sorption, indicates isotherm type and also indicates whether the sorption is favorable or not based on the following criteria: unfavorable sorption, $R_L > 1$; linear sorption, $R_L = 1$; favorable sorption, $0 < R_L < 1$; and irreversible sorption, $R_L = 0$.[48]

2.7.3. Respective contribution of surface sorption and partition to soils. The adsorption–partition model can help us understand the difference between the surface sorption and partition effect.[49] The adsorption amount of AHL at time t can be calculated as follows:

$$Q_t = Q_p + Q_a^{\max} = Kc_e + Q_a^{\max} \quad (10)$$

Here, Q_t and $Q_a^{\max}$ (mg kg^{-1}) depict the total amount of AHLs and the saturated surface sorption quantity of AHLs in soils, respectively; Q_p (mg kg^{-1}) denotes the partition amount at high AHL equilibrium concentration and K represents the partition coefficient.

2.7.4. Statistical analysis. The data analysis and processing were performed by the Origin (Version 8.5) software. The statistical data analysis of variance (ANOVA) was calculated with SPSS 21.0, and the significant level was $p < 0.05$.

3. Results and discussion

3.1. Sorption kinetics of AHLs in oxisol and alfisol

The pH values of all the sets were kept constant at 6.0 during the whole sorption period of 48 h. In the control, no significant difference was observed in the AHLs chromatography between the beginning and the end of the experiment (Fig. 1), indicating

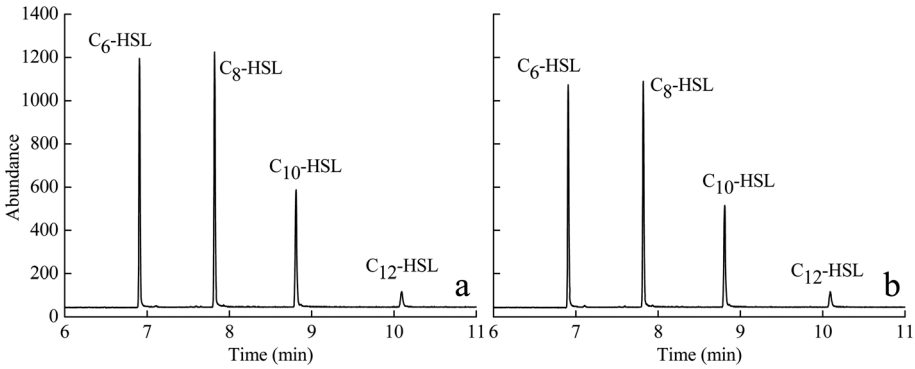

Fig. 1 Gas chromatography-mass spectrometry (GC/MS) of *N*-acyl homoserine lactones (HSLs) in the control at 0 h (a) and 48 h (b).

Open Access Article. Published on 05 March 2018. Downloaded on 10/19/2025 7:44:04 PM.
This article is licensed under a Creative Commons Attribution-NonCommercial 3.0 Unported Licence.

that chemical hydrolysis of AHLs was negligible during the sorption. Therefore, the kinetic sorption data could be fitted by three classic kinetic models.

Sorption kinetics models of the experimental data are vital to elucidate the sorption mechanism as well as the diffusion process. Rapid sorption of AHLs to soils S1 and S2 occurs during the initial 12 and 6 h, respectively. This is followed by slower

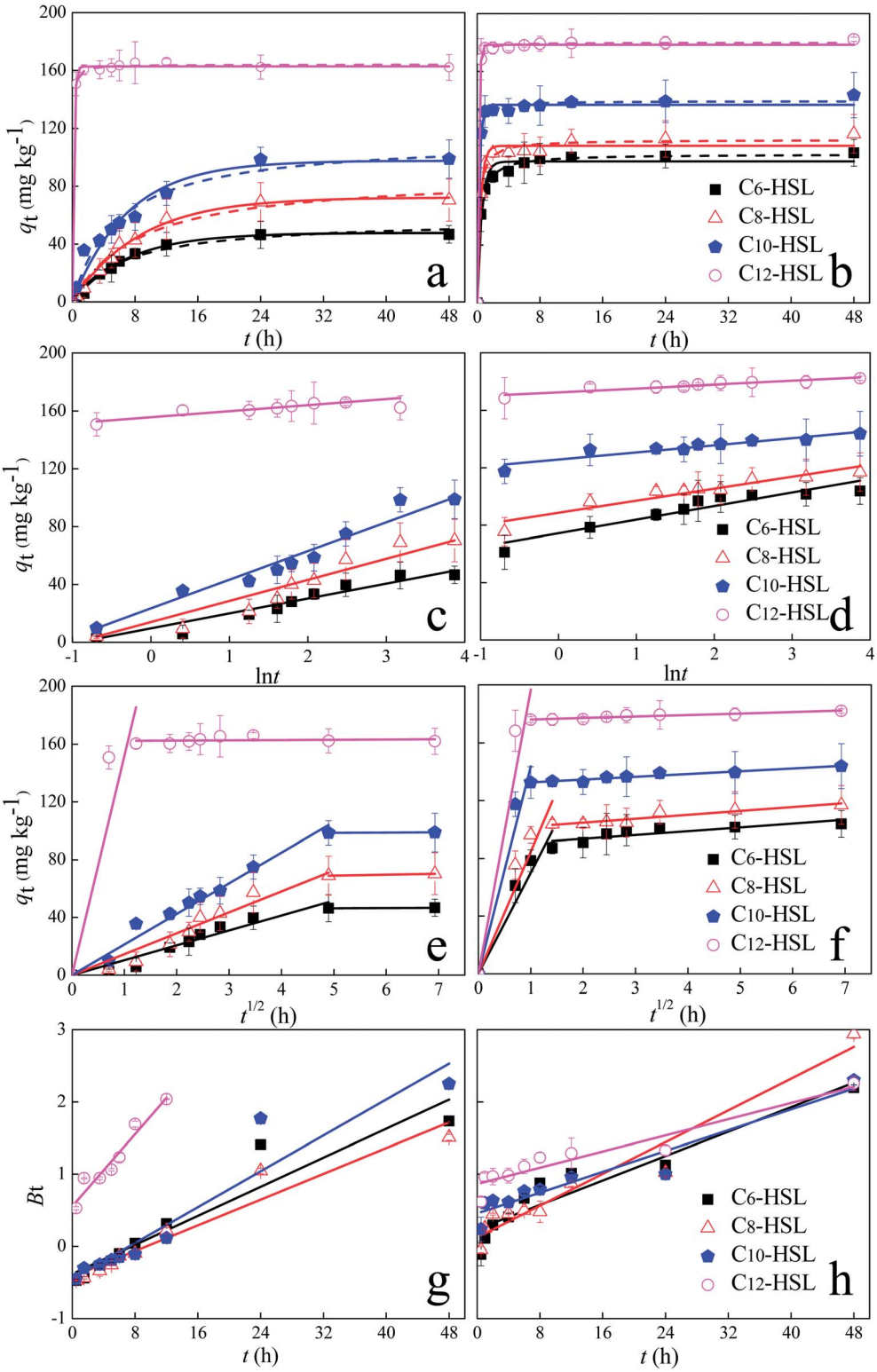

Fig. 2 Sorption kinetics of *N*-acyl homoserine lactones (HSLs) on oxisol (a, c and e) and alfisol (b, d and f). Dots: measured data; curves: pseudo-first order model (the solid curves) and pseudo-second order model (the dashed curves) (a and b); Elovich model (c and d); intra-particle diffusion model (e and f); and Boyd model (g and h).

 This journal is © The Royal Society of Chemistry 2018

Open Access Article. Published on 05 March 2018. Downloaded on 10/19/2025 7:44:04 PM.
This article is licensed under a Creative Commons Attribution-NonCommercial 3.0 Unported Licence.

Table 3 Kinetic parameters for *N*-acyl homoserine lactones (HSLs) adsorption on oxisol and alfisol

	Measured AHLs	Pseudo-first-order model			Pseudo-second-order model			Elovich model		
Treatment	$q_{e,exp}$ (mg kg^{-1})	$q_{fe,cal}$ (mg kg^{-1})	k_F (h^{-1})	R^2	$q_{se,cal}$ (mg kg^{-1})	$k_s \times 10^{-3}$ (kg mg^{-1} h^{-1}) $\times 10^{-3}$	R^2	a (mg kg^{-1})	b	R^2
Oxisol										
C_6-HSL	50.06 ± 1.10	47.67 ± 1.10	0.33 ± 0.02	0.993	56.87 ± 3.23	2.69 ± 1.02	0.977	9.65 ± 0.50	10.32 ± 0.54	0.978
C_8-HSL	75.13 ± 1.94	72.75 ± 1.94	0.27 ± 0.02	0.992	88.29 ± 5.43	1.35 ± 1.32	0.977	14.01 ± 0.87	14.61 ± 0.95	0.967
C_{10}-HSL	100.69 ± 5.56	97.72 ± 5.56	0.33 ± 0.05	0.952	112.87 ± 6.80	1.53 ± 1.00	0.968	23.51 ± 0.72	19.82 ± 0.79	0.987
C_{12}-HSL	163.96 ± 0.68	162.77 ± 0.68	12.00 ± 0.78	0.999	164.11 ± 0.67	140.79 ± 0.07	0.998	155.72 ± 0.97	4.19 ± 0.51	0.904
Alfisol										
C_6-HSL	102.17 ± 1.89	97.83 ± 1.89	4.01 ± 0.45	0.977	102.90 ± 0.80	28.51 ± 0.02	0.998	74.36 ± 2.85	9.46 ± 1.03	0.867
C_8-HSL	112.35 ± 1.77	108.66 ± 1.77	5.27 ± 0.57	0.982	112.88 ± 1.64	39.11 ± 0.03	0.991	88.60 ± 2.39	8.38 ± 1.09	0.880
C_{10}-HSL	139.44 ± 1.23	137.12 ± 1.23	8.82 ± 0.79	0.994	139.70 ± 1.17	81.53 ± 0.01	0.997	125.70 ± 1.62	4.98 ± 0.74	0.849
C_{12}-HSL	179.81 ± 0.69	178.51 ± 0.69	13.14 ± 0.91	0.999	179.94 ± 0.59	169.43 ± 0.05	1.000	172.64 ± 0.83	2.63 ± 0.38	0.855

sorption which levels off and finally reaches a plateau for S1 and S2 after 24 h and 12 h, respectively (Fig. 2a and b). The initial fast sorption can be ascribed to the presence of more accessible sites within the soil matrixes as well as the high AHLs concentration. Then a slow stage occurs in which the sorption increases slowly and reaches an equilibrium due to the increase in the number of sites occupied by the adsorbed AHLs.[50,51] There is no significant change ($p < 0.05$) in the amount of AHLs absorbed onto soils S1 between 24 h and 48 h. Hence, a contact time of 24 h is applied for further sorption isotherm experiments of AHLs onto soil S1. Similarly, for the AHLs sorption onto soil S2, 12 h is calculated as the equilibrium time.

The kinetic sorption data were fitted by three different kinetic models: the pseudo-first-order, pseudo-second-order and Elovich models (Fig. 2a–d, Table 3). The kinetic data fitted both the pseudo-first-order and pseudo-second-order models ($R^2 \geq 0.95$). Nevertheless, the pseudo-second-order model showed lower normalized standard deviation (NSD) values compared with the NSDs of the pseudo-first-order (20.07–35.64%) and Elovich models (7.69–29.88%). Overall, the pseudo-second-order models provided a more precise description of AHL sorption in soils S1 and S2, implying that chemical sorption was involved.[52,53] The equilibrium sorption amount of four AHLs on soil S1 ranged from 56.87 mg kg^{-1} to 164.11 mg kg^{-1}. For AHLs adsorbed on soil S2, the equilibrium sorption amount of AHLs was higher, ranging from 102.89 to 179.94 mg kg^{-1}.

To better understand the sorption process, the intra-particle diffusion model was applied to fit the sorption kinetic data. The sorption process of AHLs to the two soils could be divided into two stages (Fig. 2e and f), indicating that two or more steps dominate the sorption process. The first stage may be ascribed to the rapid diffusion of AHLs during external surface adsorption, representing the mass transfer of AHLs from the bulk solution.[54] Then, the sorption reached a balance at the second stage, demonstrating that it was controlled by intra-particle diffusion or pore diffusion. Besides, the linear plots of the second stage did not pass through the origin (Fig. 2e and f), indicating that the sorption process was not solely dominated by the intra-particle diffusion.[55]

The transportation process of AHLs is controlled by the film diffusion, surface diffusion, intra-particle diffusion, pore diffusion or a combination of one or two types of diffusion.

The Boyd model plots failed to pass through the origin (Fig. 2g and h), suggesting that the adsorption of AHLs onto soils was

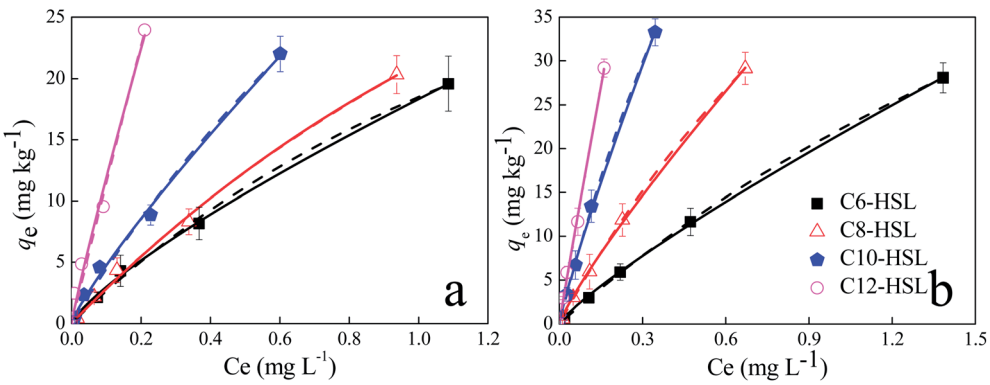

Fig. 3 Sorption isotherms of *N*-acyl homoserine lactones (HSLs) adsorbed on oxisol (a) and on alfisol (b). Dots: measured data. Lines: model fitted curves. Freundlich model (the solid lines) and Langmuir model (the dashed lines). q_e (mg kg^{-1}) is the amount of AHLs adsorbed to soils; C_e (mg L^{-1}) is the equilibrium concentration of AHLs in the solution.

Open Access Article. Published on 05 March 2018. Downloaded on 10/19/2025 7:44:04 PM.
This article is licensed under a Creative Commons Attribution-NonCommercial 3.0 Unported Licence.

Table 4 Isotherm parameters of *N*-acyl homoserine lactones (HSLs) sorption onto oxisol and alfisol

	Langmuir model			Freundlich model			
Treatment	q_m (mg kg^{-1})	k_L (L mg^{-1})	R^2	k_F (mg kg^{-1}) (mg L^{-1})$^{-n}$	n	ΔG (kJ mol^{-1})	R^2
Oxisol							
C_6-HSL	55.15 ± 9.38	0.50 ± 0.49	0.997	18.33 ± 0.26	0.79 ± 0.02	−7.21 ± 3.37	0.999
C_8-HSL	75.23 ± 20.22	0.39 ± 0.89	0.997	21.39 ± 0.38	0.84 ± 0.03	−7.59 ± 2.37	0.998
C_{10}-HSL	99.85 ± 50.35	0.47 ± 1.34	0.994	33.61 ± 1.41	0.85 ± 0.05	−8.27 ± 0.85	0.995
C_{12}-HSL	197.75 ± 290.51	0.65 ± 2.53	0.988	97.76 ± 19.70	0.91 ± 0.11	−11.36 + 7.39	0.981
Alfisol							
C_6-HSL	101.14 ± 3.45	0.28 ± 0.16	0.999	21.40 ± 0.17	0.84 ± 0.01	−7.59 ± 4.44	0.999
C_8-HSL	114.34 ± 4.94	0.51 ± 0.11	0.999	41.19 ± 0.55	0.86 ± 0.02	−9.22 ± 1.50	0.999
C_{10}-HSL	141.03 ± 9.74	0.89 ± 0.10	0.999	84.31 ± 2.65	0.87 ± 0.02	−10.99 ± 2.42	0.998
C_{12}-HSL	263.39 ± 89.85	0.77 ± 0.49	0.994	168.54 ± 13.15	0.96 ± 0.04	−12.71 ± 6.39	0.999

mainly governed by a diffusion-controlled mechanism based on the film.

3.2. Sorption isotherm of AHLs

The experimentally obtained isothermal data best fitted the Freundlich model (the solid curves of Fig. 3; Table 4) and the Langmuir model (the dot curves of Fig. 3; Table 4), indicating that the monolayer sorption and heterogeneous energetic distribution of active sites on the surface of the soils occurred during the sorption process, which involved chemical and physical sorption.[48] According to the Langmuir model, the sorption capacities (q_m) of S2 were higher than those of S1, which may be ascribed to different physiochemical properties of the soils. For both soils, the nonlinear exponent, n, was close to 1.0, indicating that the sorption of AHL to these soils was favorable and dominated by the partition effect (Table 4).[50] Additionally, the adsorption–partition model was calculated to further separate surface sorption from partition sorption. The partition sorption of AHLs on the two soils accounted for at

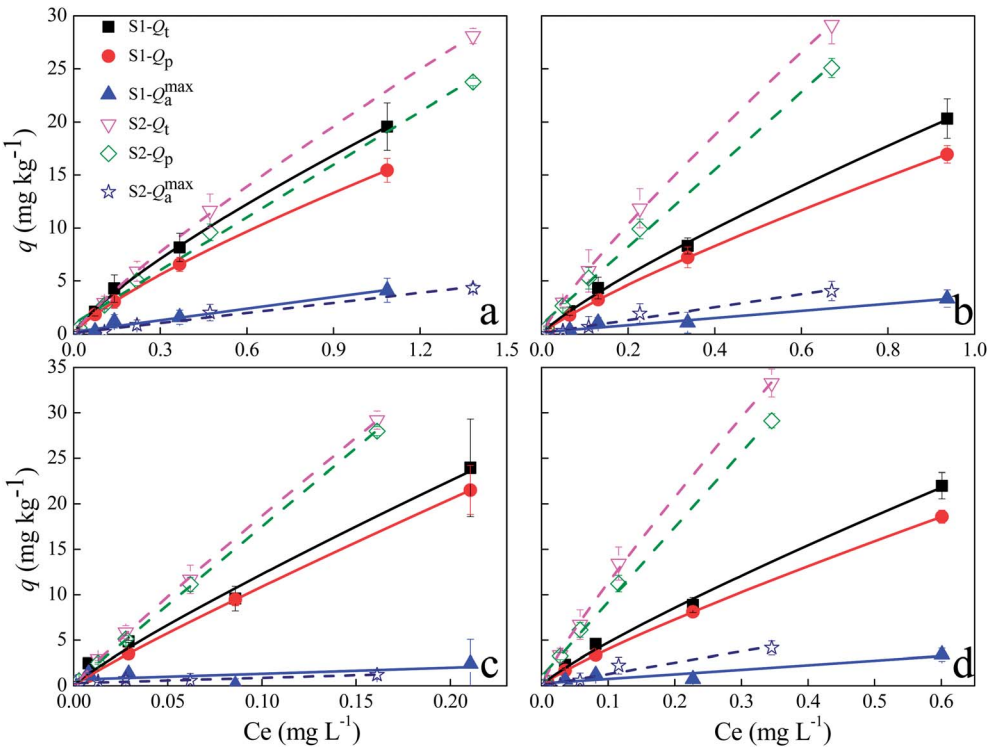

Fig. 4 Respective contributions of partition (Q_p) and surface sorption (Q_a^{max}) to total sorption (Q_t) of *N*-acyl homoserine lactones (C_6-HSL, (a); C_8-HSL, (b); C_{10}-HSL, (c); C_{12}-HSL, (d) to oxisol (S1-solid lines) and alfisol (S2-dot line)). Q_t (mg kg^{-1}) is the total amount of AHLs that sorbed to the soil; Q_a^{max} (mg kg^{-1}) represents the surface sorption quantity of AHLs to soils; Q_p (mg kg^{-1}) denotes the partition amount of AHLs; C_e (mg L^{-1}) is the equilibrium concentration of AHLs in the solution.

Open Access Article. Published on 05 March 2018. Downloaded on 10/19/2025 7:44:04 PM.
This article is licensed under a Creative Commons Attribution-NonCommercial 3.0 Unported Licence.

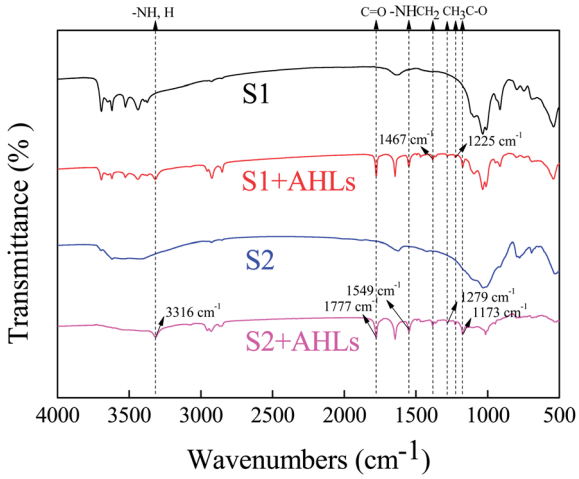

Fig. 5 FTIR spectra of oxisol (S1) and alfisol (S2) before and after sorption of four kinds of *N*-acyl homoserine lactones (AHLs).

least 72% over the test range (Fig. 4). Additionally, the thermodynamic parameter, Gibbs free energy (ΔG), values ranged from −7.21 to 12.71 kJ mol^{-1} (Table 4), implying that the sorption of AHLs may be dominated by physical sorption.[50,56] The R_L values of AHLs adsorbed by the soils ranged from 0.18 to 0.42, revealing that the sorption of AHLs on the two soils was favorable, which agreed well with the Freundlich model.

3.3. FTIR analysis

The soil surface functional groups were analyzed with FTIR before and after sorption of AHLs. Very similar vibrational features were expected for all AHLs due to their analogous molecular structures.[57] The spectra were dominated by six strong bonds at 3311, 1777, 1644, 1551, 1175 and 1025 cm^{-1}, which could be assigned to the characteristic vibrations of the amide and lactone functional groups.[57] After the sorption of AHLs on the two soils, the 3311 cm^{-1} band shifted to 3316 cm^{-1}, the band at 1644 cm^{-1} disappeared and the peak at 1549 cm^{-1} remained unchanged (Fig. 5), and these peaks could be easily assigned to the key vibrations of the amide group, *i.e.*, ν(N–H), amide I, and amide II,[58–60] respectively. The 1777 cm^{-1} band remained unchanged and was representative of the lactone C=O stretch, ν(C=O). Four small weak peaks appeared at 1467, 1279, 1225 and 1173 cm^{-1}. The peak at 1467 cm^{-1} was ascribed to bending vibrations of aliphatic CH_2 and CH_3, and the other three peaks were ascribed to C–O vibration.[58] These results indicated that carbonyl, amide, CH_2 and CH_3 bonds might take part in the AHLs sorption to the two kinds of soils. Thus, AHLs might be adsorbed on soils by the electrostatic interaction between the positively charged groups (–NH) and the negatively charged adsorption sites, which is similar to the adsorption of tetracycline on soil.[61] Therefore, we could conclude that the electrostatic forces and hydrogen bonding might influence the adsorption of AHLs on these two soils.

3.4. Relationship of sorption parameters with AHLs properties

With regards to different AHLs, the structure and presence of certain functional groups might be the main factors influencing their adsorption behaviors. In this study, the relations of the four sorption parameters (q_e, q_m, k_F, and $1/n$) with AHLs properties

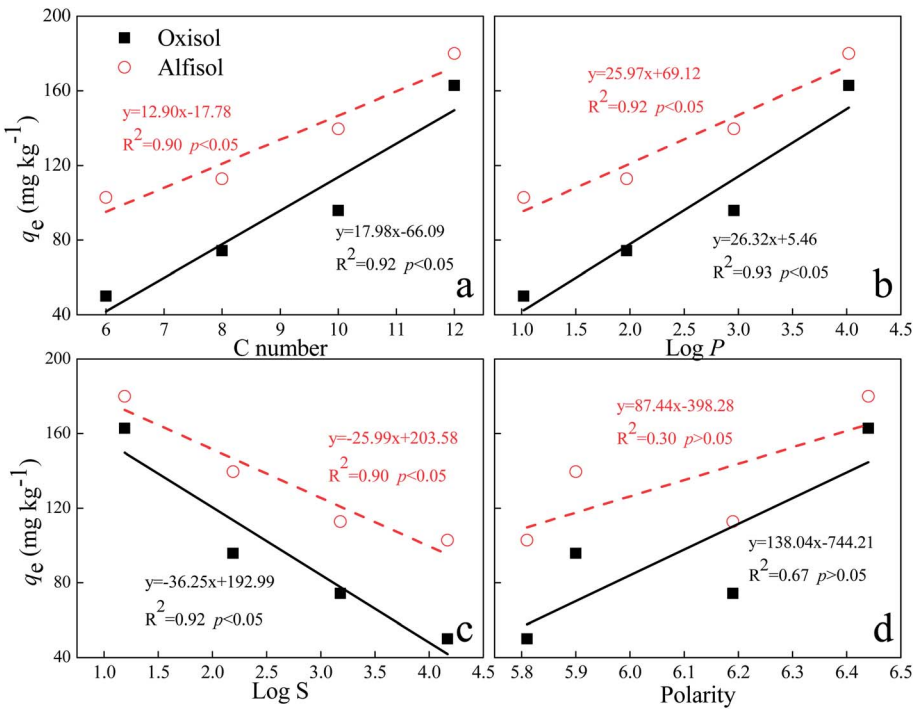

Fig. 6 Relationships between equilibrium sorption amount of soil (q_e) and the number of C molecules in the side chain (a), log *P* (b), log *S* (c) and polarity (d) of *N*-acyl homoserine lactones in oxisol and alfisol.

Open Access Article. Published on 05 March 2018. Downloaded on 10/19/2025 7:44:04 PM.
This article is licensed under a Creative Commons Attribution-NonCommercial 3.0 Unported Licence.

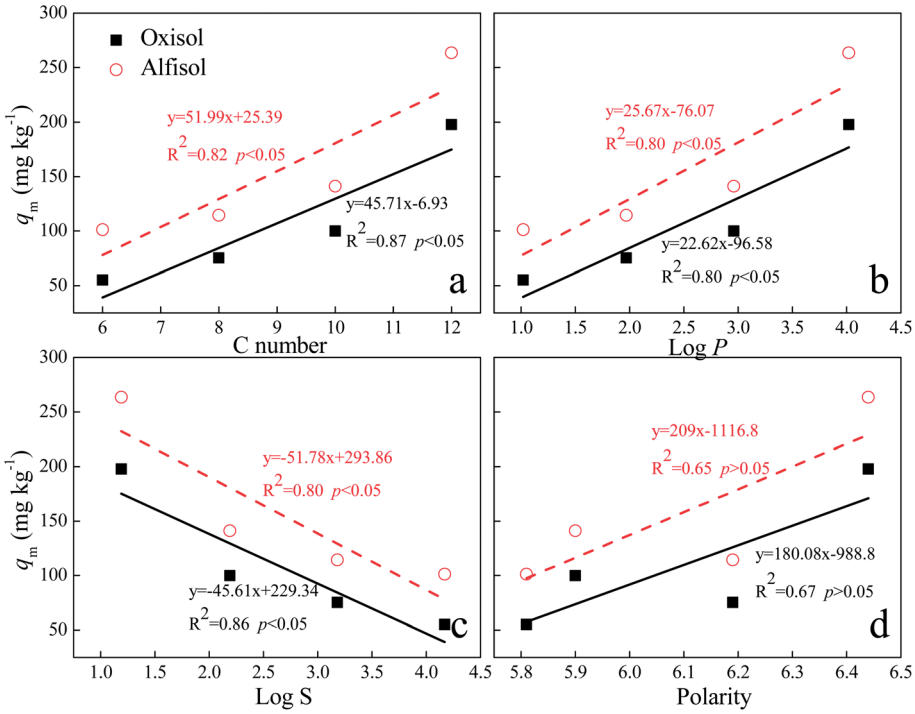

Fig. 7 Relationships between q_m and the number of C molecules in the side chain (a), log P (b), log S (c) and polarity (d) of N-acyl homoserine lactones in oxisol and alfisol.

were investigated. The equilibrium sorption amount of AHLs (q_e) positively correlated with the log P value and the length of the acyl side chain of each AHL (Fig. 6). With the increase in log P or the length of acyl side chain, there was a corresponding increase in q_e of AHLs: C_{12}-HSL > C_{10}-HSL > C_8-HSL > C_6-HSL. In contrast, log S (which stands for the logarithm of water solubility) of each AHL showed a negative correlation with q_e. Please note that although the q_e values increased with the polarities of AHLs, there were no obvious correlations between the polarities and the q_e values of AHLs (Fig. 6), which was different from the adsorption of AHLs on soil particles.[29]

For the Langmuir equation model, there is a similar correlation between the maximum sorption (q_m) and the physicochemical properties (length of acyl side chain, log P, log S and polarity) (Fig. 7), indicating that the maximum sorption capacity of AHLs may also be influenced by their structure, log P and water solubility. Nevertheless, there are no obvious correlations between the values of K_L and the physicochemical characteristics of AHLs. Additionally, the contribution of the surface sorption effect decreases for both soil types with the increasing length of the acyl side chain, which is confirmed by the increased n values (Table 4). The sorption capacity of the soils (k_F) also increase in the following order: C_6-HSL < C_8-HSL < C_{10}-HSL < C_{12}-HSL (Table 4) for both soil types. Nevertheless, no obvious correlation exists between k_F and the physicochemical properties of AHLs.

4. Conclusions

The sorption kinetics and isotherms of AHLs in natural soils were analyzed to provide insights into the sorption of AHLs as a function of AHLs and the physicochemical properties of the soil. Physical and chemical characteristics, such as molecular structure, solubility speciation and log P, as well as the properties of the soils were responsible for the adsorption characteristics of QS molecules in the soils. AHL sorption onto the two soils was mainly governed by a film diffusion-controlled mechanism. The partition effect dominated the sorption of AHLs to the soils, suggesting that electrostatic forces and hydrogen bonding are involved in AHL sorption to soils. These findings clearly illustrated that sorption is an important environmental process controlling the transportation and diffusion of AHLs, especially in acidic soils, implying a potential challenge for quorum sensing in the soil environment.

Conflicts of interest

There are no conflicts to declare.

Acknowledgements

This study was financially supported by the Outstanding Youth Fund of Natural Science Foundation of Jiangsu, China (BK20150050), National Science and Technology Major Project of China (2016YFD0800204), the National Key Basic Research Program of China (2014CB441105), the National Natural Science Foundation of China (21677149, 21277148) and the Key Program of Frontier Sciences, Chinese Academy of Sciences (QYZDJ-SSW-DQC035).

References

1 P. Williams, *Microbiology*, 2007, **153**, 3923–3938.

Open Access Article. Published on 05 March 2018. Downloaded on 10/19/2025 7:44:04 PM.
This article is licensed under a Creative Commons Attribution-NonCommercial 3.0 Unported Licence.

2 A. W. Decho, R. S. Norman and P. T. Visscher, *Trends Microbiol.*, 2010, **18**, 73–80.
3 C. M. Waters and B. L. Bassler, *Cell Dev. Biol.*, 2005, **21**, 28–346.
4 S. Atkinson and P. Williams, *J. R. Soc., Interface*, 2009, **6**, 20.
5 M. B. Miller and B. L. Bassler, *Annu. Rev. Microbiol.*, 2001, **55**, 165–199.
6 Z. Bulman, A. Hudson and M. A. Savka, *FASEB J.*, 2011, **25**(suppl. 1), 948.1.
7 G. Chong, O. Kimyon and M. Manefield, *PLoS One*, 2013, **8**, e67443.
8 B. L. Bassler and R. Losick, *Cell*, 2006, **125**, 237–246.
9 N. R. Thomson, M. A. Crow, S. J. McGowan, A. Cox and G. P. C. Salmond, *Mol. Microbiol.*, 2000, **36**, 539–556.
10 R. Van Houdt, P. Moons, A. Aertsen, A. Jansen, K. Vanoirbeek, M. Daykin, P. Williams and C. W. Michiels, *Res. Microbiol.*, 2007, **158**, 150–158.
11 N. J. Bainton, B. W. Bycroft, S. R. Chhabra, P. Stead, L. Gledhill, P. J. Hill, C. E. D. Rees, M. K. Winson, G. P. C. Salmond, G. S. A. B. Stewart and P. Williams, *Gene*, 1992, **116**, 87–91.
12 A. Nickzad, F. Lepine and E. Deziel, *PLoS One*, 2015, **10**, e0128509.
13 A. Alagely, C. J. Krediet, K. B. Ritchie and M. Teplitski, *ISME J.*, 2011, **5**, 1609–1620.
14 A. L. Kim, S.-Y. Park, C.-H. Lee, C.-H. Lee and J.-K. Lee, *J. Microbiol. Biotechnol.*, 2014, **24**, 1574–1582.
15 H. Sheng, M. Harir, L. A. Boughner, X. Jiang, P. Schmitt-Kopplin, R. Schroll and F. Wang, *Sci. Total Environ.*, 2017, **605–606**, 1031–1038.
16 F. Wang, A. Fekete, M. Harir, X. Chen, U. Dörfler, M. Rothballer, X. Jiang, P. Schmitt-Kopplin and R. Schroll, *Chemosphere*, 2013, **92**, 1403–1409.
17 A. W. Decho, R. L. Frey and J. L. Ferry, *Chem. Rev.*, 2011, **111**, 86–99.
18 L. V. Rinaudi and W. Giordano, *FEMS Microbiol. Lett.*, 2010, **304**, 1–11.
19 C. d'Angelo-Picard, D. Faure, I. Penot and Y. Dessaux, *Environ. Microbiol.*, 2005, **7**, 1796–1808.
20 J. J. Huang, A. Petersen, M. Whiteley and J. R. Leadbetter, *Appl. Environ. Microbiol.*, 2006, **72**, 1190–1197.
21 S. Uroz, C. Angelo-Picard, A. Carlier, M. Elasri, C. Sicot, A. Petit, P. Oger, D. Faure and Y. Dessaux, *Microbiology*, 2003, **149**, 1981–1989.
22 S. Uroz, Y. Dessaux and P. Oger, *ChemBioChem*, 2009, **10**, 205–216.
23 G. F. Kaufmann, R. Sartorio, S.-H. Lee, C. J. Rogers, M. M. Meijler, J. A. Moss, B. Clapham, A. P. Brogan, T. J. Dickerson and K. D. Janda, *Proc. Natl. Acad. Sci. U. S. A.*, 2005, **102**, 309–314.
24 E. A. Yates, B. Philipp, C. Buckley, S. Atkinson, S. R. Chhabra, R. E. Sockett, M. Goldner, Y. Dessaux, M. Cámara, H. Smith and P. Williams, *Infect. Immun.*, 2002, **70**, 5635–5646.
25 Y. J. Wang and J. R. Leadbetter, *Appl. Environ. Microbiol.*, 2005, **71**, 1291–1299.
26 X. Feng, A. J. Simpson and M. J. Simpson, *Org. Geochem.*, 2005, **36**, 1553–1566.
27 P. A. Meyers and J. G. Quinn, *Geochim. Cosmochim. Acta*, 1973, **37**, 1745–1759.
28 J. R. Bartlett and H. E. Doner, *Soil Biol. Biochem.*, 1988, **20**, 755–759.
29 P. L. Liu, X. Chen and W. L. Chen, *Geomicrobiol. J.*, 2015, **32**, 602–608.
30 X. Gao, H.-Y. Cheng, I. Del Valle, S. Liu, C. A. Masiello and J. J. Silberg, *ACS Omega*, 2016, **1**, 226–233.
31 C. A. Masiello, Y. Chen, X. D. Gao, S. Liu, H. Y. Cheng, M. R. Bennett, J. A. Rudgers, D. S. Wagner, K. Zygourakis and J. J. Silberg, *Environ. Sci. Technol.*, 2013, **47**, 11496–11503.
32 M. Englmann, A. Fekete, C. Kuttler, M. Frommberger, X. Li, I. Gebefügi, J. Fekete and P. Schmitt-Kopplin, *J. Chromatogr. A*, 2007, **1160**, 184–193.
33 C. Santi, G. Certini and L. P. D'Acqui, *Commun. Soil Sci. Plant Anal.*, 2006, **37**, 155–162.
34 L.-F. Alfonso, G. V. Germán, P. C. María del Carmen and G. Hossein, *Chemosphere*, 2017, **166**, 292–299.
35 H. Sheng, Y. Song, Y. Bian, W. Wu, L. Xiang, G. Liu, X. Jiang and F. Wang, *Anal. Methods*, 2017, **9**, 688–696.
36 S. Uroz, P. Oger, S. R. Chhabra, M. Cámara, P. Williams and Y. Dessaux, *Arch. Microbiol.*, 2006, **187**, 249–256.
37 X. Chen, K. Buddrus-Schiemann, M. Rothballer, P. M. Kramer and A. Hartmann, *Anal. Bioanal. Chem.*, 2010, **398**, 2669–2676.
38 L. Delalande, D. Faure, A. Raffoux, S. Uroz, C. D'Angelo-Picard, M. Elasri, A. Carlier, R. Berruyer, A. Petit, P. Williams and Y. Dessaux, *FEMS Microbiol. Ecol.*, 2005, **52**, 13–20.
39 M. Jia, F. Wang, Y. Bian, X. Jin, Y. Song, F. O. Kengara, R. Xu and X. Jiang, *Bioresour. Technol.*, 2013, **136**, 87–93.
40 S. Lagergren, *K. Sven. Vetenskapsakad. Handl.*, 1898, **24**, 1–39.
41 Y. S. Ho and G. McKay, *Process Biochem.*, 1999, **34**, 451–465.
42 C. Aharoni and F. C. Tompkins, *Adv. Catal.*, 1970, **21**, 1–49.
43 N. Kannan and M. M. Sundaram, *Dyes Pigm.*, 2001, **51**, 25–40.
44 G. E. Boyd, A. W. Adamson and L. S. Myers, *J. Am. Chem. Soc.*, 1947, **69**, 2836–2848.
45 H. Freundlich, *Z. Phys. Chem., Stoechiom. Verwandtschaftsl.*, 1906, **57**, 385–470.
46 I. Langmuir, *J. Am. Chem. Soc.*, 1916, **38**, 2221–2295.
47 G. McKay, H. S. Blair and J. R. Gardner, *J. Appl. Polym. Sci.*, 1982, **27**, 3043–3057.
48 J. Zhang, C. Wu, A. Jia and B. Hu, *Appl. Surf. Sci.*, 2014, **298**, 95–101.
49 B. Chen, D. Zhou and L. Zhu, *Environ. Sci. Technol.*, 2008, **42**, 5137–5143.
50 G. Liu, Y. Bian, M. Jia, L. A. Boughner, C. Gu, Y. Song, H. Sheng, W. Zhao, X. Jiang and F. Wang, *Sci. Total Environ.*, 2017, **609**, 144–152.
51 D. Feng, H. M. Yu, H. Deng, F. Z. Li and C. J. Ge, *BioResources*, 2015, **10**, 6751–6768.

Open Access Article. Published on 05 March 2018. Downloaded on 10/19/2025 7:44:04 PM.
This article is licensed under a Creative Commons Attribution-NonCommercial 3.0 Unported Licence.

52 C. P. Chen, W. J. Zhou, Q. Yang, L. F. Zhu and L. Z. Zhu, *Chem. Eng. J.*, 2014, **240**, 487–493.
53 Y. S. Ho, *J. Hazard. Mater.*, 2006, **136**, 681–689.
54 K. Y. Foo and B. H. Hameed, *Bioresour. Technol.*, 2013, **130**, 696–702.
55 B. H. Hameed, I. A. W. Tan and A. L. Ahmad, *Chem. Eng. J.*, 2008, **144**, 235–244.
56 V. Vimonses, S. Lei, B. Jin, C. W. K. Chow and C. Saint, *Chem. Eng. J.*, 2009, **148**, 354–364.
57 J. Bak and J. Spanget-Larsen, *Vib. Spectrosc.*, 2009, **49**, 237–241.
58 W. V. Gerasimowicz, D. M. Byler and H. Susi, *Appl. Spectrosc.*, 1986, **40**, 504–507.
59 D. Bhaduri, A. Saha, D. Desai and H. N. Meena, *Chemosphere*, 2016, **148**, 86–98.
60 S. Kim, S. W. Won, C.-W. Cho and Y.-S. Yun, *Desalin. Water Treat.*, 2016, **57**, 20084–20090.
61 R. A. Figueroa, A. Leonard and A. A. MacKay, *Environ. Sci. Technol.*, 2004, **38**, 476–483.

 This journal is © The Royal Society of Chemistry 2018